Global and Planetary Change 92–93 (2012) 267–274

Contents lists available at SciVerse ScienceDirect

Global and Planetary Change

journal homepage: www.elsevier.com/locate/gloplacha

Coastal marsh die-off and reduced attenuation of coastal floods: A model analysis

Stijn Temmerman [a,*], Mindert B. De Vries [b], Tjeerd J. Bouma [c]

[a] Ecosystem Management Research Group, Department of Biology, University of Antwerp, Universiteitsplein 1, 2610 Antwerp, Belgium
[b] Deltares Delft Hydraulics, Rotterdamseweg 185, 2629 HD Delft, The Netherlands
[c] Royal Netherlands Institute for Sea Research (NIOZ Yerseke), POB 140, 4400 AC Yerseke, The Netherlands

ARTICLE INFO

Article history:
Received 24 October 2011
Accepted 5 June 2012
Available online 13 June 2012

Keywords:
coastal flooding
flood mitigation
salt marshes
ecosystem services
storm surge
sea level rise

ABSTRACT

Global climate change is expected to increase the risks of coastal flood disasters due to accelerating sea level rise and increasing intensity and frequency of storm surges. Coastal marsh vegetation is considered, on the one hand, to increase resistance to a landward propagating flood wave, such as a storm surge, and hence to protect against flood disasters. On the other hand, coastal marsh vegetation is dying off at several places around the world due to accelerating sea level rise. Here we present hydrodynamic model simulations of flood attenuation by a tidal marsh, with particular focus on the effects of spatial patterns of vegetation die-off. It is shown that a same percentage of marsh die-off but occurring as different spatial patterns of marsh break-up has largely different effects on flood attenuation. Patches of die-off that are directly connected to tidal channels have a much greater effect on increased landward flood propagation, while a same percentage of marsh die-off, but occurring at inner marsh locations disconnected from tidal channels, has only a minor effect. This implies that a random pattern of up to 50% of marsh die-off still provides a considerable flood attenuating effect. However with increasing percentage of random marsh die-off the flood attenuating effect decreases exponentially, since the chance for vegetation die-off occurring directly adjacent to tidal channels increases. This study demonstrates that tidal marsh die-off, which may increase with ongoing global change, is expected to have non-linear effects on reduced coastal protection against flood waves.

1. Introduction

Global climate change is expected to increase the risks and impact of coastal flooding in the coming century, through accelerating sea level rise (Meehl et al., 2005; Jevrejeva et al., 2010), increasing frequency and intensity of storm surges (Emanuel, 2005; Webster et al., 2005), and growing coastal populations (Nicholls and Cazenave, 2010). Today an estimated 10 million people experience coastal flooding each year, and this number could increase to 50 million by 2080 due to global change (Nicholls, 2004). Hence there is an urgent need for sustainable strategies to cope with the growing risks of coastal flooding.

Coastal wetland ecosystems, such as tidal marshes and mangroves, are increasingly identified as natural protective barriers against coastal flooding: their dense vegetations increase resistance to a landward propagating flood wave and hence reduce inland flood water levels (e.g., Costanza et al., 2008; Das and Vincent, 2009; Krauss et al., 2009; Wamsley et al., 2010). Vast areas of tidal marshes and mangroves naturally occur along low-lying coasts and in large deltas, which are exactly those places in the world that are most vulnerable to coastal flooding (Nicholls and Cazenave, 2010).

Human and natural pressure has led, however, to rapid global-scale degradation and loss of tidal marshes (ca. 50%) and mangrove ecosystems (ca. 35%) over the past two to three decades (Alongi, 2002; Millennium Ecosystem Assessment, 2005). Large-scale die-off of marsh vegetation may occur, with conversion into bare tidal flats or shallow water, as a consequence of processes such as marsh submergence by sea level rise (Baumann et al., 1984; Kearney et al., 2002; Marani et al., 2007; Kirwan et al., 2010) and herbivore grazing (e.g., Silliman et al., 2005). Hence the large-scale die-off of marsh vegetation may result in a drastic decrease of the protection provided by tidal marshes against coastal flooding. For that reason, extensive marsh conservation and restoration programs were proposed recently. For example, in the wake of the devastating hurricane Katrina surge that flooded New Orleans in 2005, about 2 billion U.S.$ have been nominated to restore 1000 s of acres of tidal marshes that previously submerged in the Mississippi deltaic area, with the intention to attenuate the landward propagation of storm surges caused by the passage of tropical cyclones (Stokstad, 2005; Day et al., 2007).

Despite such plans, remarkably little scientific knowledge exists on the relationships between tidal marsh characteristics, such as the degree of marsh die-off, and their effects on the attenuation of a landward propagating flood wave. This lack of knowledge is largely attributed to the scarcity and heterogeneity of field measurements of extreme flood water levels within and behind large tidal wetlands. The relatively few field data that exist display a wide range of flood

* Corresponding author.
E-mail address: stijn.temmerman@ua.ac.be (S. Temmerman).

0921-8181/$ – see front matter © 2012 Elsevier B.V. All rights reserved.
doi:10.1016/j.gloplacha.2012.06.001

attenuation rates, ranging from about 4 to 25 cm of flood level reduction per kilometer of tidal wetland (Lovelace, 1994; Krauss et al., 2009; Wamsley et al., 2010). This wide range suggests that the extent of flood level reduction is highly variable between specific wetland locations and between specific flood events.

Hydrodynamic modeling studies have recently enlarged our insights on the mitigating effect of coastal marshes on extreme floods during storm surges. Especially storm surge simulations for the U.S. Gulf coastal area, which were performed after the hurricane Katrina surge (2005), have demonstrated that enhanced friction by coastal marshes can slow down the landward propagation of storm surges, which increases peak water levels seaward of the marsh, and reduces peak water levels landward at rates that are within the values reported from observations (e.g., Resio and Westerink, 2008; Westerink et al., 2008; Wamsley et al., 2009). Model simulations further revealed that the attenuation rate is not constant but may strongly vary, depending on the specific geometry and bathymetry of the coastal zone, and on the intensity, duration, and track of the storm forcing (Wamsley et al., 2010). Moderate storm surges (with peak water depth 2 to 3 m above the marshes) are most effectively attenuated by coastal marshes, while extremely high storm surges (5 m and more) that continue longer may be so overwhelming that coastal marshes have a relatively smaller attenuating effect (Loder et al., 2009; Wamsley et al., 2010). Simulations further demonstrated that the attenuating effect decreases when degradation of coastal marsh vegetation is simulated (by using lower friction values), when a higher bed elevation in the coastal marsh zone is applied, and when straight wide channels are considered within the marsh (Loder et al., 2009; Wamsley et al., 2009, 2010).

While these modeling studies emphasized on simulating the physical processes that generate a storm surge for large coastal landscape settings (e.g., Loder et al., 2009; Wamsley et al., 2009, 2010), their maximum grid resolutions of approximately 200 m was too rough to account for the spatial complexity of vegetation patterns that are typical for tidal marshes. As a consequence vegetation die-off was simulated in the storm surge models as rather spatially homogenous over larger marsh areas (Wamsley et al., 2009), while field observations show that vegetation die-off is typically occurring on specific localized portions of the marsh platform, resulting in a heterogeneous break-up of the marsh vegetation by gradual emergence of bare patches (e.g., Kearney et al., 2002; Kearney and Rogers, 2010). Furthermore, vegetation die-off is generally considered to result in a local reduction of sediment deposition or even bed erosion, leading in the longer term to a decrease of the local bed elevation relative to rising sea level (e.g., Morris et al., 2002; Marani et al., 2007; Kirwan et al., 2010). In the present study we specifically address the high-resolution (20 m) effects of spatial patterns of vegetation die-off, with and without the combination of bed lowering, on the rate of flood attenuation.

Our choice for a high-resolution hydrodynamic model approach implied to simplify the hydrodynamic forcing, by simulating the propagation of an externally-forced sinusoidal flood wave over a tidal marsh. Hence it is not our intention to include the simulation of storm surge formation at the open ocean off-shore from coastal marshes, which would necessitate to include complex effects of wind friction, wave piling, and atmospheric pressure setup in generating the storm surge (e.g., Resio and Westerink, 2008; Westerink et al., 2008). An externally-applied flood wave, as simulated in the present study, can be considered as a reasonable approximation when focusing on high-resolution effects of spatial patterns of vegetation die-off on flood attenuation, as wind friction, wave piling, and atmospheric pressure setup are expected to have little effect once the flood wave travels through a tidal marsh.

As a first objective, we study the effect of different percentages of vegetation die-off, occurring as different spatial patterns of marsh break-up, on the amount of flood wave attenuation. As a second objective, we investigate the combined effect of patterns of vegetation die-off and local sediment bed lowering on flood wave attenuation. These two objectives are addressed by hydrodynamic model simulations of flood propagation through a tidal marsh.

2. Methods

2.1. Brief model description

Flood wave propagation through a tidal marsh was simulated using the DELFT3D-FLOW model. This hydrodynamic model computes flow characteristics, such as flow velocities and water level changes, over a two- or three-dimensional finite difference grid, based on the Shallow-Water equations (Hydraulics, 2003; Lesser et al., 2004). In previous studies the model has been calibrated and validated against field data on tidal water level changes and flow velocities in a Dutch tidal salt marsh (Temmerman et al., 2005, 2007). In the present study the model was applied in two-dimensional (2D) mode, in accordance with previous modeling studies assuming that three-dimensional effects on flood propagation through tidal marshes are of minor importance (Loder et al., 2009; Wamsley et al., 2009, 2010). When applied in 2D mode, friction is simulated using a roughness coefficient that is considered here to be representative for friction exerted by both the sediment bed surface and by the vegetation canopy. A Chezy-type roughness formulation is used, with the Chezy roughness coefficient, C, defined as $C = H^{1/6}.n^{-1}$, where H = water depth [m] and n = the Manning roughness coefficient [$m^{-1/3}$.s]. Hence the used friction factor is dependent on water depth and on a predefined Manning n-value, as in previous models for storm surge propagation through coastal marshes (Loder et al., 2009; Wamsley et al., 2009, 2010).

2.2. Model implementation

We performed simulations of flood wave propagation over a rectangular grid representing an idealized coastal zone of 2 km alongshore length and 200 km cross-shore length, of which 20 km of tidal marsh and 180 km of off-shore coastal zone (Fig. 1). The large off-shore zone was included in order to allow the simulation of inertia effects on the piling up of water levels against the seaward edge of the marsh zone, which was found to be a significant process in previous modeling studies of storm surge propagation over tidal marshes (Loder et al., 2009; Wamsley et al., 2009, 2010). Horizontal grid cells were 20×20 m within the marsh zone, while gradually larger grid cells (up to 1000×20 m) were used in off-shore direction. A time-step of three seconds was applied.

The off-shore bathymetry was schematized as a regular off-shore slope of 1:1000 (Fig. 1), in accordance with recent simulations (Loder et al., 2009) that were designed to be representative for storm surge mitigation by coastal marshes in Louisiana. The marsh zone was defined as a flat platform dissected by a branched network of tidal channels (Fig. 1A). The marsh platform had an elevation of 0.5 m above mean sea level (similar to Loder et al. (2009)). At the seaward marsh edge there is a step-change in elevation of 0.5 m (Fig. 1B), which is typically found at the transition from mature tidal marshes to the non-vegetated intertidal or subtidal zone (e.g., Fagherazzi et al., 2006). The channel network was extracted from aerial pictures from a Dutch salt marsh (Fig. 1A), and reveals a dendritic channel network that may be considered as typical for non-degraded tidal marshes (e.g., Fagherazzi et al., 1999). Channels smaller than the width of a grid cell (i.e., 20 m) were not represented in the model. The bathymetry within the channels was defined as a concave length profile (Fig. 1B). Based on empirical observations and model simulations on tidal channel morphologies (see De Swart and Zimmerman (2009) for a review), both concave and convex length profiles may be found depending on factors such as tidal forcing. Hence, as mentioned also in the next paragraph, the effect of a concave versus convex channel length profile was simulated as one of the model scenarios. The

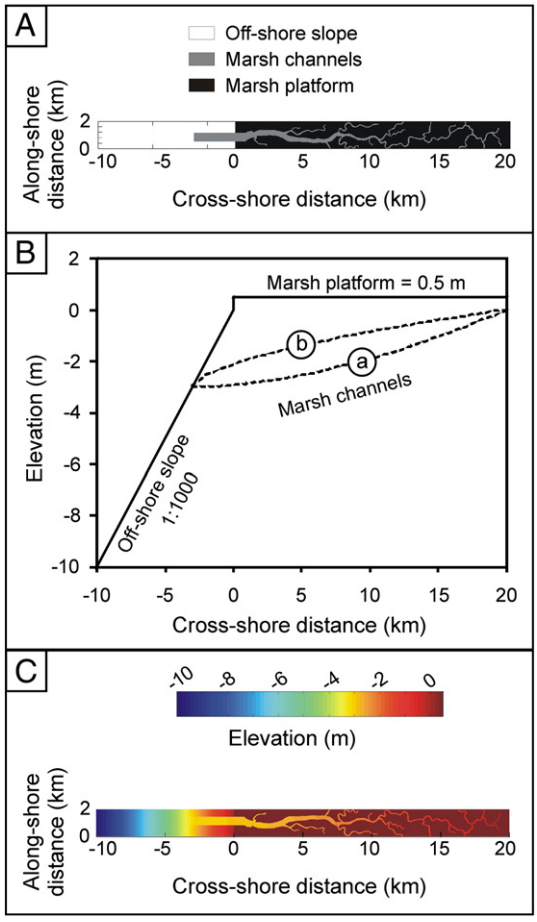

Fig. 1. (A) Map of model domain with location of the three morphological zones, i.e. the off-shore slope, the marsh platform, and marsh channels. (B) Cross-shore bathymetric profile showing the input bathymetry for the off-shore slope (1:1000), the marsh platform (elevation = 0.5 m above sea level), and marsh channels (a: concave profile used in runs 1–7 and runs 9–22; b: convex profile used in run 8). (C) Map of input bathymetry used for runs 1–22.

depth of the channels at the seaward inlet was defined at 3 m below mean sea level (Fig. 1).

On the marsh platform the effect of vegetation on friction needs to be considered. This is done by using a lower Manning *n*-value of 0.02 in the non-vegetated areas (off-shore and in the channels), which is representative for bare sand, and using a higher Manning *n*-value for the vegetated marsh platform. A definitive quantification of the Manning *n*-value that is most representative to describe the roughness of a tidal marsh surface is not available from the existing literature. Previous hydrodynamic modeling studies of storm surge propagation over tidal marshes found that a Manning *n*-value of around 0.08 was resulting in simulated flood attenuation rates that corresponded well to observed flood attenuation rates (Loder et al., 2009; Wamsley et al., 2009, 2010). In accordance with these previous studies, we used a Manning *n*-value of 0.08 on the vegetated marsh platform (see Table 1: runs 4–22). In order to assess the sensitivity of the model output to the marsh Manning *n*-value, we also compared simulations with a marsh Manning *n*-value varying between 0.04, 0.08 and 0.12 (see Table 1: runs 1–3). The hydrodynamic forcing was defined as a sinusoidal water level-time function at the off-shore open boundary of the grid. A sine function was applied with a wave height of 2.5 m (i.e., minimum water level = 0 m = mean sea level; maximum water level = 2.5 m) and a wave period of 745 min, which would be representative for a storm tide (i.e., storm surge coinciding with a semi-diurnal tide). Simulations of one single flood wave were run, starting from minimum water level (= 0 m) and an initially flat water surface level of 0 m defined over the entire grid (i.e., the marsh platform is still dry). The simulations were stopped when the flood wave had flooded the entire marsh zone, more specifically as soon as water levels started to drop on all locations above the marsh platform, so that peak water levels could be computed over the entire marsh.

Table 1
Overview of model runs and input values for key model variables. For non-vegetated areas of the model grid, a Manning *n*-value of 0.02 was used (representative for bare sand).

Run ID	Channel bathymetry	Vegetation Manning *n*	Vegetation pattern		Died-off platform elevation
			Die-off (%)	Die-off (where?)	(m)
1	Concave	0.04	0	–	–
2	Concave	0.08	0	–	–
3	Concave	0.12	0	–	–
4	No channels	–	100	Complete	0.5
5	No channels	0.08	0	–	–
6	Concave	0.08	0	–	–
7	Concave	–	100	Complete	0.5
8	Convex	0.08	0	–	–
9	Concave	0.08	50	Far from channels	0.5
10	Concave	0.08	50	Along channels	0.5
11	Concave	0.08	50	Random_1	0.5
12	Concave	0.08	50	Random_2	0.5
13	Concave	0.08	50	Random_3	0.5
14	Concave	0.08	50	Random_4	0.5
15	Concave	0.08	50	Random_5	0.5
16	Concave	0.08	50	Far from channels	0.3
17	Concave	0.08	50	Along channels	0.3
18	Concave	0.08	50	Random_1	0.3
19	Concave	0.08	10	Random_1	0.5
20	Concave	0.08	30	Random_1	0.5
21	Concave	0.08	70	Random_1	0.5
22	Concave	0.08	90	Random_1	0.5

2.3. Model runs

Table 1 summarizes the different model scenarios that were run and presented in this paper. Runs 1–3 were performed to assess the sensitivity of the model simulations to the Manning *n*-value used for the vegetated marsh platform, by varying the marsh Manning *n*-value between 0.04 (run 1), 0.08 (run 2) and 0.12 (run 3). As argued above, subsequent runs 4–22 were all carried out with a marsh Manning *n*-value of 0.08, which was found to be representative for tidal marshes in previous modeling studies of storm surge propagation (Loder et al., 2009; Wamsley et al., 2009, 2010). Runs 4–7 demonstrate the general effects of the marsh vegetation and marsh channels on flood wave attenuation. Run 6, with a concave length profile of the channel bed, is compared to run 8, with a convex channel profile (see Fig. 1 for the input channel profiles). Runs 9–22 show the effects of die-off of the marsh vegetation, under different scenarios of spatial patterns of marsh die-off (runs 9–15), of vegetation die-off combined with platform bed lowering (runs 16–18), and of different percentages of the area of marsh die-off (runs 19–22).

3. Results

3.1. General effects of marsh platform, vegetation and channels

Before describing the novel findings of this paper, i.e. the non-linear effects of spatial patterns of vegetation die-off, we start with demonstrating the general effects of the marsh platform morphology, and of the presence or absence of marsh vegetation and marsh

channels. For all runs, the applied flood wave (2.5 m high at 180 km off-shore of the marsh zone) first propagates over the off-shore sloping bathymetry, resulting in a gradual landward setup of the flood wave up to about 3.8 m high at the seaward edge of the marsh zone. Run 4 demonstrates how further landward flood wave propagation is affected by the marsh platform morphology, by considering a marsh zone that consists of a flat platform (at 0.5 m elevation; Fig. 1B) without the presence of channels nor vegetation (Table 1). For this run 4, the peak water level generated by the flood wave decreases almost linearly over the marsh platform at a rate of 0.1 m/km in the landward direction (Fig. 2). Near the landward boundary of the model, there is a setup of peak water level against the closed landward boundary.

Run 5 considers a completely vegetated marsh platform, without any channels (Table 1), and shows that the vegetation-induced friction results in a much faster decrease of peak water level in the landward direction, at an almost linear rate of 0.26 m/km (Fig. 2). Run 5 also shows that the vegetation-induced friction results in slightly higher peak water levels (as compared to run 4) seaward of the marsh and within the first 1.4 km of the marsh, as a consequence of the inertia of the flood propagation and the reduced propagation speed as soon as the flood wave enters the marsh vegetation.

Run 6 includes both the presence of vegetation and channels in the marsh zone (Table 1; channel pattern as in Fig. 1), and demonstrates the combined vegetation effect on slower flood propagation over the marsh platform, and the channel effect on concentration and facilitation of flood propagation through the channels, resulting in a more complex non-linear reduction of peak water level in the landward direction (Fig. 2). On average the peak water level is reduced with 0.08 m/km within the first 10 km of the marsh, and with 0.22 m/km within the next 5 km of the marsh. Run 7 shows only the effect of the channels without presence of marsh vegetation (Table 1), illustrating the channel effect on facilitation of the landward flood wave propagation.

When comparing runs 1–3 with different Manning *n*-values for the vegetated zones, it is demonstrated that with increasing vegetation friction the landward flood propagation is increasingly reduced, while this is also associated with an increasing piling up of water level at the seaward edge of the marsh (Fig. 3). Using a convex length profile for the channel bed (run 8) or a concave profile (run 6) (see Fig. 1 for the length profiles), it is shown that a reduction of channel depth, as in the convex profile, slows down the flood propagation and causes a faster landward decrease of peak water level (Fig. 4).

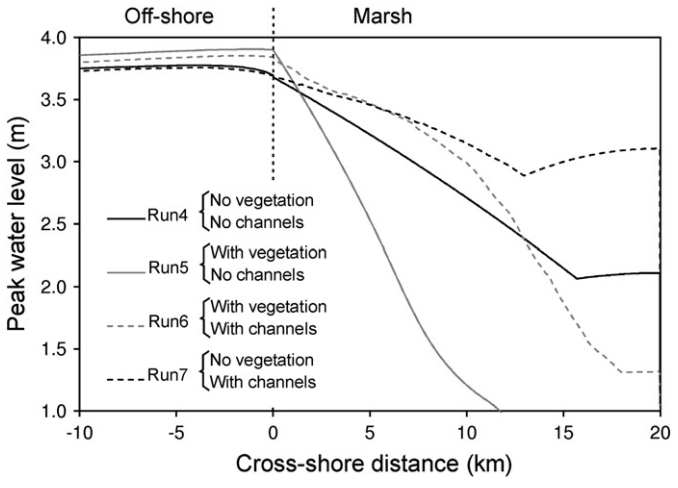

Fig. 2. Influence of marsh platform morphology, presence or absence of marsh vegetation, and of channels, on simulated peak water levels along the cross-shore transect. Run 4, without vegetation or channels. Run 5, with vegetation but without channels. Run 6, with vegetation and with channels. Run 7, with channels but without vegetation. Water level and marsh surface level are expressed to the same reference level (mean sea level). For more detailed info on model input values see Table 1.

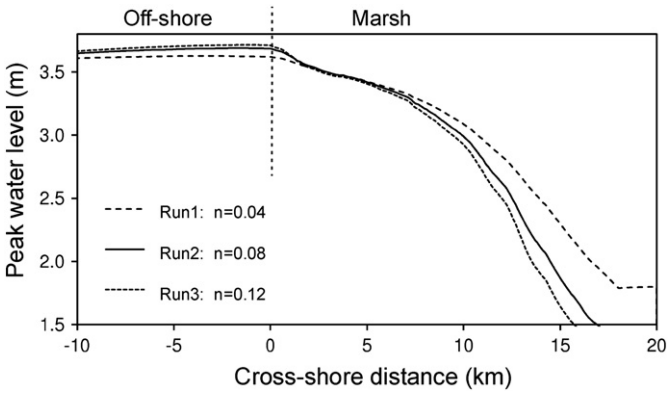

Fig. 3. Influence of Manning *n*-value. Run 1, $n=0.04$. Run 2, $n=0.08$. Run 3, $n=0.12$. For more info on input values see Table 1.

3.2. Effects of spatial patterns of vegetation die-off

Runs 9–15 allow the comparison of vegetation die-off over 50% of the marsh platform but occurring in different spatial patterns. In run 9 all of the die-off has occurred in the so-called inner marsh portions far away and disconnected from the marsh channels (Fig. 5). This results in faster flood flow velocities above the inner marsh portions where vegetation has disappeared (Fig. 6), hence more landward flood propagation and increased peak water levels that are 0.15 to 0.4 m higher over most of the marsh zone, as compared to run 6 with a fully vegetated marsh platform (Fig. 5). In run 10 all of the vegetation die-off has taken place directly along the marsh channels (Fig. 5), leading to concentrated flow and accelerated flood propagation within and along the marsh channels (Fig. 6). As a result the increase of peak water levels becomes increasingly important in the landward direction, with peak water levels that are up to 0.8 m higher than when a full vegetation cover is present (run 6) (Fig. 5). Hence an equal amount of marsh die-off (50%) has a markedly stronger effect on increased landward flood propagation when the vegetation die-off occurs in marsh portions directly connected to the channels (run 10), as compared to vegetation die-off in marsh zones separated from the channels by an intermediate vegetated zone (run 9).

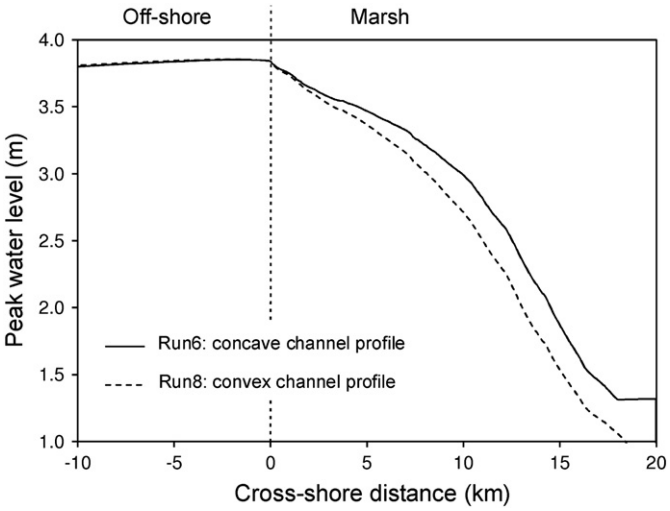

Fig. 4. Influence of channel bed length profile on simulated peak water levels. Run 6, concave length profile (a in Fig. 1B). Run 8, convex length profile (b in Fig. 1B). For more info on input values see Table 1.

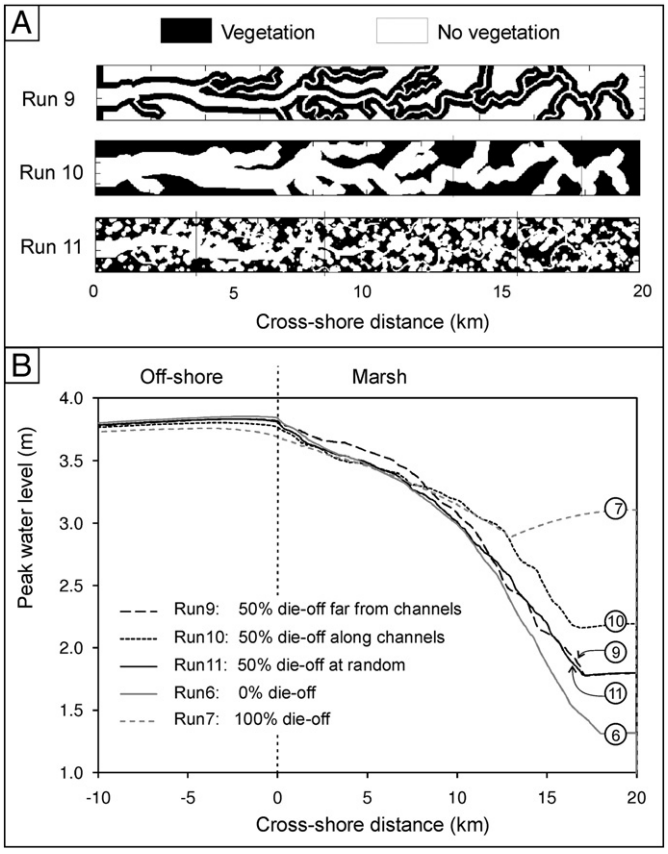

Fig. 5. Influence of vegetation die-off over 50% of the marsh area but occurring in different patterns. The vegetation patterns are shown in panel A. The simulated peak water levels are shown in panel B. Run 9, 50% die-off far from channels. Run 10, 50% die-off along channels. Run 11, 50% die-off at random. Run 6, 0% die-off. Run 7, 100% die-off (absence of vegetation). For more info on input values see Table 1.

Run 11 simulates then a random pattern of vegetation die-off, with more or less circular bare patches that may occur either right along the channels or disconnected from the channels (Fig. 5). Such a random die-off pattern has apparently few effects on peak water levels within the first 10 km of the marsh (Fig. 5). Accordingly, the flow velocities are not so strongly accelerated in the bare patches within the first 10 km, while farther inland faster flow velocities occur (Fig. 6) and an increasing peak water level is simulated up to 0.35 m higher than with full vegetation presence (Fig. 5). Runs 11 to 15, with different random patterns of 50% of vegetation die-off, demonstrate that depending on the pattern the simulated peak water level may vary locally as much as 0.15 m (Fig. 7).

The combination of marsh die-off with lowering of the platform elevation with 0.2 m relative to mean sea level (as to simulate the longer term effect of marsh die-off on decreased sedimentation or even erosion), resulted in simulated peak water levels (runs 16 to 18) that were only slightly different from the peak water levels simulated without considering bed lowering (runs 9 to 11) (Fig. 8).

Finally, with increasing percentage of died-off marsh area (runs 19 to 22), the peak water level is not so much affected in the first 7.5 km of the marsh, but is increasingly heightened further inland (Fig. 9). It is highlighted that the peak water level increases non-linearly but rather exponentially with increasing percentage of marsh die-off (Figs. 9 and 10). This is because with increasing percentage of marsh die-off, the chance for random bare patches to be directly connected to the channel network is increasing (Fig. 9). Hence, with increasing random marsh die-off the flood attenuating effect is found to decrease exponentially (Fig. 10).

4. Discussion

Global change, in particular accelerating sea level rise, is causing the patchy die-off and break-up of tidal marsh vegetation at many places around the world (e.g., Baumann et al., 1984; Kearney et al., 2002; Kirwan et al., 2010), and this is generally considered to reduce the flood attenuating effect of tidal marshes (e.g., Day et al., 2007; Wamsley et al., 2009, 2010). This study demonstrates that especially the spatial pattern of marsh die-off rather than the aerial extent of die-off is determinant for the flood attenuating effect of tidal marshes. Died-off patches that are directly connected to tidal channels have a much greater effect on increased landward flood propagation, while a same percentage of marsh die-off, but occurring at locations far away and disconnected from tidal channels, has only a minor effect (Figs. 5 and 6). This implies that with increasing percentage of random marsh die-off the flood attenuating effect decreases exponentially, since the chance for vegetation die-off occurring directly adjacent to tidal channels increases (Figs. 9 and 10). Hence this study demonstrates that tidal marsh die-off, which may increase with ongoing global change, leads to a non-linear but exponential reduction of the protective function of tidal marshes against coastal flood events.

Our simulated rates of flood attenuation by tidal marshes agree with the range of values that were previously observed and simulated for storm surges. Our simulated attenuation rates – for marshes with 0 to 50% of die-off (Fig. 5) – range between 0.06 and 0.09 m/km for the first 10 km of marsh, and between 0.15 and 0.23 m/km for the next 5 km. These values match with the range of storm surge attenuation rates that have been reported from measured data (0.04 to 0.25 m/km; (Lovelace, 1994; Krauss et al., 2009; Wamsley et al., 2010)) and from storm surge modeling for coastal Louisiana (0.02

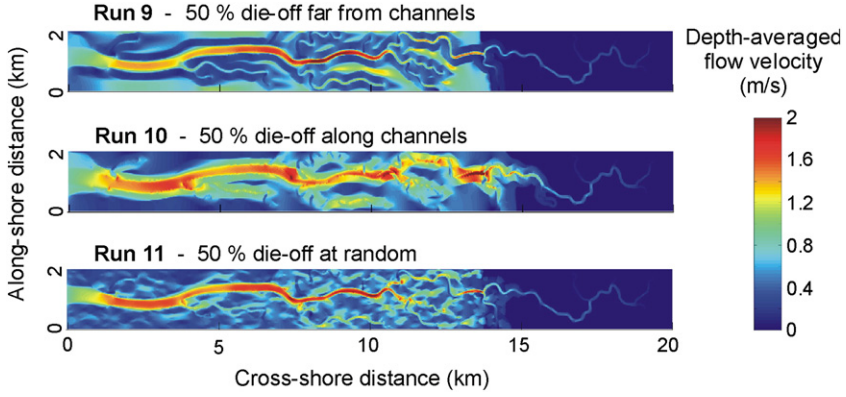

Fig. 6. Maps of depth-averaged flow velocity patterns simulated for different patterns of 50% of vegetation die-off. The vegetation patterns are shown in Fig. 5A. Run 9, 50% die-off far from channels. Run 10, 50% die-off along channels. Run 11, 50% die-off at random.

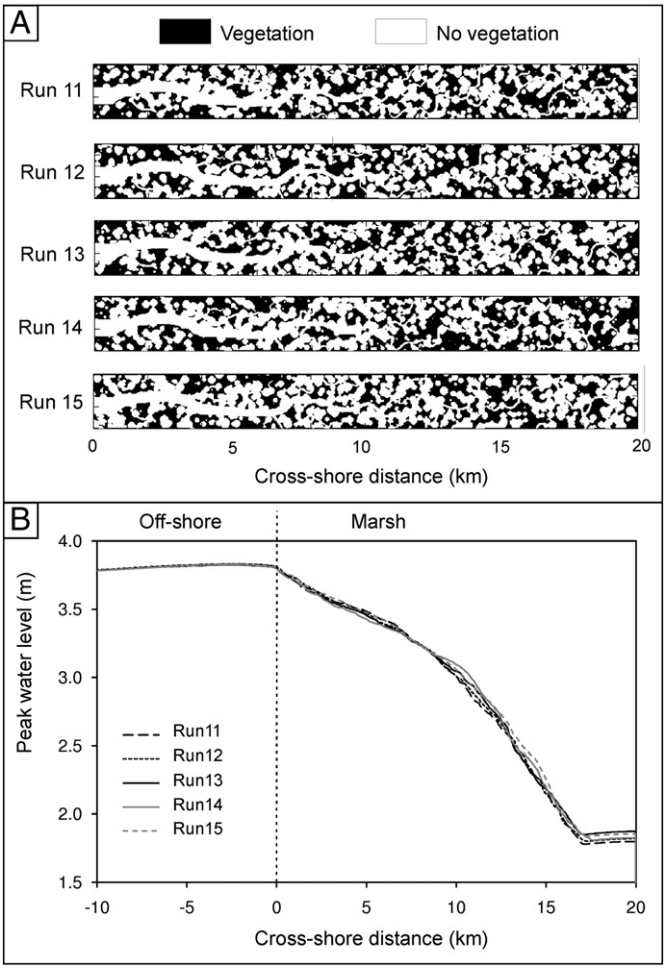

Fig. 7. Influence of different random patterns (runs 11–15) of 50% of vegetation die-off. The vegetation patterns are shown in panel A. The simulated peak water levels are shown in panel B. For info on input values see Table 1.

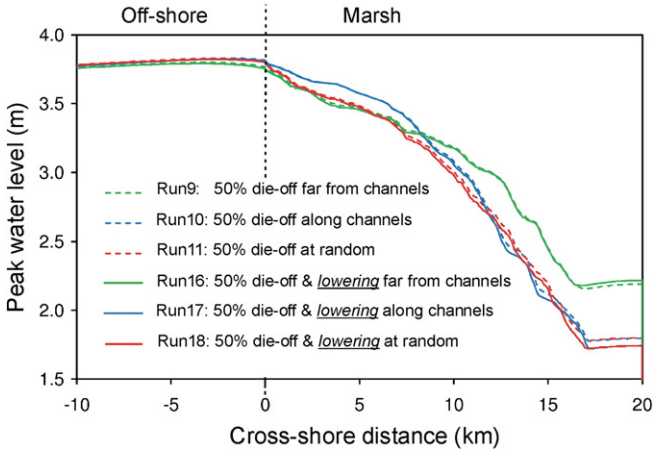

Fig. 8. Influence of the combination of vegetation die-off and bed lowering (with 0.2 m) in the died-off areas, on simulated peak water levels. The die-off patterns are shown in Fig. 5A. Runs 9 and 16, 50% die-off far from channels without and with bed lowering. Runs 10 and 17, 50% die-off along channels without and with bed lowering. Runs 11 and 18, 50% die-off at random without and with bed lowering. For more info on input values see Table 1.

to 0.17 m/km (Wamsley et al., 2010)). The general effects of the marsh platform morphology (landward reduction of peak water levels), marsh vegetation (additional landward reduction and seaward heightening of peak water levels), and marsh channels (facilitated landward propagation) that were simulated with our model approach (Fig. 2) are also consistent with simulations by storm surge models (Loder et al., 2009; Wamsley et al., 2009, 2010). This indicates that our simplification of using an externally-applied flood wave, instead of simulating the generation of a storm surge within the model domain, was not a major constraint for the relevance of our simulations. Once a storm surge enters a tidal marsh, the further built up by wind friction, waves and atmospheric pressure effects is indeed expected to be restricted, while friction exerted by the marsh vegetation and morphology is expected to control the flood propagation. In contrast with existing storm surge simulations that used a quite rough spatial resolution (~200 m) within the marsh domain (Loder et al., 2009; Wamsley et al., 2009, 2010), our simplified hydrodynamic forcing did enable us to use a high-resolution (20 by 20 m), which allowed simulating the effects of complex spatial patterns of marsh die-off.

Existing studies that quantified the spatial patterns of tidal marsh die-off are relatively scarce (e.g., Kearney and Rogers, 2010), but suggest that marsh die-off preferentially occurs in lower marsh portions (depressions) that are located further away from channels, while the relatively higher located natural levees closer to the channels, are less vulnerable to vegetation die-off. Our study demonstrates that such a pattern of marsh die-off, which is concentrated at inner marsh locations further away and disconnected from the tidal channels (e.g. as in Fig. 7 run 9), would have a relatively small effect on landward flood propagation. In this case the flood propagation is not so much accelerated because the flood wave still feels friction from the vegetated marsh zones in between the channels and the bare inner marsh portions, so that the increase of flood flow velocities in the bare inner marsh zones is rather limited (Fig. 6). However, when the same percentage of marsh die-off would occur in direct connection with the channel network, increased flow velocities occur over the died-off marsh platform, leading to much faster inland flood propagation (Fig. 6). This mechanism implies that, when considering a random pattern of increasing percentage of marsh die-off, the degree of flood attenuation decreases exponentially with the percentage of marsh die-off (Fig. 10). This is because for low percentages of die-off, the chance for random bare patches to be directly connected to the channel network is low, and this chance is increasing for increasing percentages of died-off marsh area (Fig. 9). Hence, it is very likely that a marsh that has died-off for up to 50% still provides a considerable flood attenuating effect, but with increasing marsh die-off this attenuating effect would decrease exponentially.

The die-off of marsh vegetation is likely to result also in changes in marsh morphology in the longer term. Vegetation die-off is widely considered to reduce the local deposition of organic and mineral sediment (e.g., Mudd et al., 2010) and to cause in the longer term a lowering of the bed elevation relative to rising sea level (e.g., Morris et al., 2002; Marani et al., 2007; Kirwan et al., 2010). Here we simulated the effect of platform lowering with 0.2 m at died-off spots, which would be representative for a sediment accretion deficit relative to rising sea level after a few to several decades in most coastal marshes (Kirwan et al., 2010). This bed lowering of 0.2 m had only a very minor additional effect on the simulated flood attenuation (Fig. 8). Hence marsh die-off is expected to have an immediate effect on reduced flood attenuation through the removal of the vegetation-induced friction.

This study highlights the importance of studying the spatial patterns of marsh die-off with accelerating sea level rise, in order to assess the effects of global change on the ecosystem services provided by coastal marshes. Although there is a rapidly growing understanding of the general environmental conditions under which coastal marsh submergence is likely to occur (e.g. Kirwan et al., 2010), the spatial patterns of marsh break-up have been comparatively poorly studied (e.g., Kearney and Rogers, 2010). Furthermore, it may be deduced from this study that complex interactions between marsh break-up and increased marsh flooding may be expected. As marshes

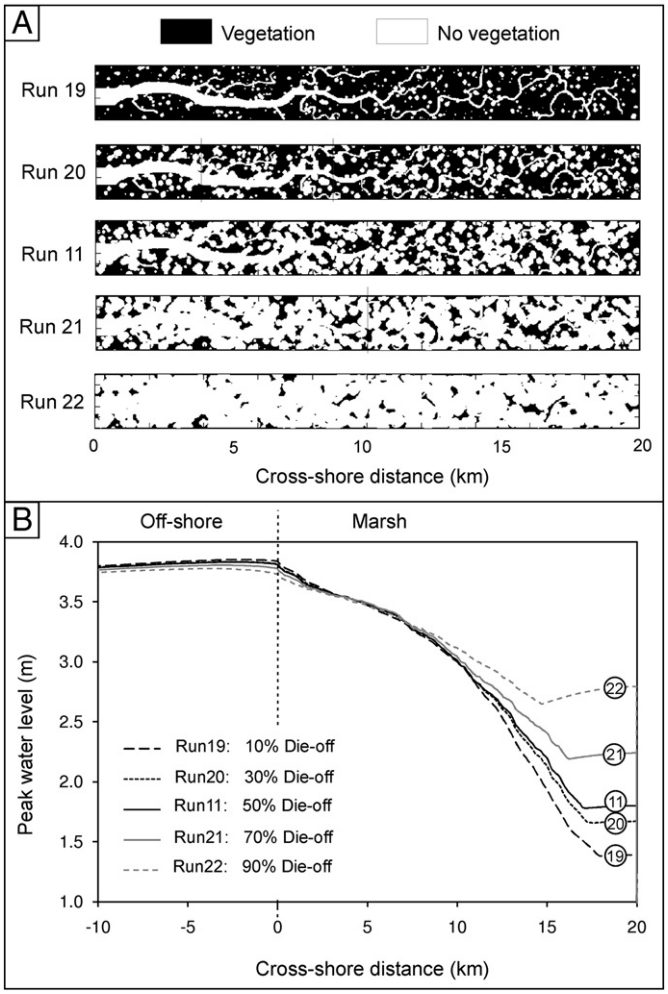

Fig. 9. Influence of increasing percentage of vegetation die-off. The random die-off patterns are shown in panel A. The simulated peak water levels are shown in panel B. Run 19, 10% die-off. Run 20, 30% die-off. Run 11, 50% die-off. Run 21, 70% die-off. Run 22, 90% die-off. For more info on input values see Table 1.

gradually break-up, the reduction of the vegetation-induced friction is expected to cause increased landward propagation of extreme floods but also of the normal tidal floodings, which would cause increased inundation stress for the remaining marsh vegetation and which may ultimately lead to a runwaway feedback towards complete permanent marsh loss. Therefore we conclude that the causes and consequences of coastal marsh die-off should be studied with a particular attention for the spatial processes and patterns involved.

5. Conclusions

This study presented hydrodynamic model simulations of the landward propagation of an externally-forced coastal flood wave and the attenuating effect of tidal marshes, highlighting the importance of the patchy spatial patterns of vegetation die-off. The following conclusions can be drawn:

(1) Vegetation die-off, occurring over a same percentage of the marsh area but as different spatial patterns of vegetation break-up, have considerably different effects on flood wave attenuation. Especially died-off bare patches that make direct connection with the marsh channels, have a much greater effect on increased landward flood propagation than bare patches that are disconnected from the channels by intermediate zones of marsh vegetation.

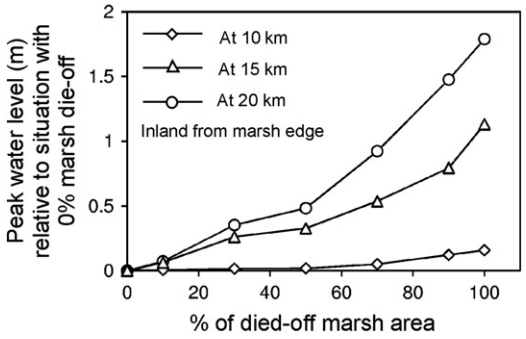

Fig. 10. Non-linear exponential effect of increasing percentage of vegetation die-off on increasing inland peak flood water levels, at 10 km (diamonds), 15 km (triangles), and 20 km (balls) inland from the marsh edge.

(2) This mechanism implies that the degree of flood attenuation decreases exponentially with increasing percentage of random marsh break-up. This is because for low percentages of die-off, the chance for random bare patches to be directly connected to the channel network is low, while this chance is increasing for increasing percentages of died-off marsh area. Hence, a marsh that has died-off for up to 50% is likely to provide still a considerable flood attenuating effect, but with increasing marsh die-off this attenuating effect would decrease exponentially.

(3) The lowering of the marsh platform relative to sea level, which is associated in the longer term with vegetation die-off as a consequence of reduced sedimentation or even erosion, is shown to have only a minor additional effect on landward flood propagation.

Acknowledgments

We thank Deltares Delft Hydraulics for use of the DELFT3D-FLOW model, and are especially grateful to M. Van Ormondt and F. Dekker for early discussions that stimulated this work.

References

Alongi, D.M., 2002. Present state and future of the world's mangrove forests. Environmental Conservation 29, 331–349.
Baumann, R.H., Day, J.W., Miller, C.A., 1984. Mississippi deltaic wetland survival: sedimentation versus coastal submergence. Science 224, 1093–1095.
Costanza, R., Perez-Maqueo, O., Martinez, M.L., Sutton, P., Anderson, S.J., Mulder, K., 2008. The value of coastal wetlands for hurricane protection. Ambio 37, 241–248.
Das, S., Vincent, J.R., 2009. Mangroves protected villages and reduced death toll during Indian super cyclone. Proceedings of the National Academy of Sciences of the United States of America 106, 7357–7360.
Day, J.W., Boesch, D.F., Clairain, E.J., Kemp, G.P., Laska, S.B., Mitsch, W.J., Orth, K., Mashriqui, H., Reed, D.J., Shabman, L., Simenstad, C.A., Streever, B.J., Twilley, R.R., Watson, C.C., Wells, J.T., Whigham, D.F., 2007. Restoration of the Mississippi delta: lessons from hurricanes Katrina and Rita. Science 315, 1679–1684.
De Swart, H.E., Zimmerman, J.T.F., 2009. Morphodynamics of tidal inlet systems. Annual Review of Fluid Mechanics 41, 203–229.
Emanuel, K., 2005. Increasing destructiveness of tropical cyclones over the past 30 years. Nature 436, 686–688.
Fagherazzi, S., Bortoluzzi, A., Dietrich, W.E., Adami, A., Lanzoni, S., Marani, M., Rinaldo, A., 1999. Tidal networks 1. Automatic network extraction and preliminary scaling features from digital terrain maps. Water Resources Research 35, 3891–3904.
Fagherazzi, S., Carniello, L., D'Alpaos, L., Defina, A., 2006. Critical bifurcation of shallow microtidal landforms in tidal flats and salt marshes. Proceedings of the National Academy of Sciences of the United States of America 103, 8337–8341.
Hydraulics, W.D., 2003. User Manual Delft3D-FLOW. WL | Delft Hydraulics, Delft, The Netherlands.
Jevrejeva, S., Moore, J.C., Grinsted, A., 2010. How will sea level respond to changes in natural and anthropogenic forcings by 2100? Geophysical Research Letters 37, L07703.
Kearney, M.S., Rogers, A.S., 2010. Forecasting sites of future coastal marsh loss using topographical relationships and logistic regression. Wetlands Ecology and Management 18, 449–461.
Kearney, M.S., Rogers, A.S., Townshend, J.R.G., Stevenson, J.C., Stevens, J., Rizzo, E., Sundberg, K., 2002. Landsat imagery shows decline of coastal marshes in Chesapeake and Delaware Bays. EOS Transactions of the American Geophysical Union 83, 173–178.

Kirwan, M.L., Guntenspergen, G.R., D'Alpaos, A., Morris, J.T., Mudd, S.M., Temmerman, S., 2010. Limits on the adaptability of coastal marshes to rising sea level. Geophysical Research Letters 37, L23401.

Krauss, K.W., Doyle, T.W., Doyle, T.J., Swarzenski, C.M., From, A.S., Day, R.H., Conner, W.H., 2009. Water level observations in mangrove swamps during two hurricanes in Florida. Wetlands 29, 142–149.

Lesser, G.R., Roelvink, J.A., Van Kester, J.A.T.M., Stelling, G.S., 2004. Development and validation of a three-dimensional morphological model. Coastal Engineering 51, 883–915.

Loder, N.M., Irish, J.L., Cialone, M.A., Wamsley, T.V., 2009. Sensitivity of hurricane surge to morphological parameters of coastal wetlands. Estuarine, Coastal and Shelf Science 84, 625–636.

Lovelace, J.K., 1994. Storm-tide Elevations Produced by Hurricane Andrew along the Louisiana Coast, August 25–27, 1992. Open File Report 94-371. Geological Survey, Baton Rouge, LA, U.S.

Marani, M., D'Alpaos, A., Lanzoni, S., Carniello, L., Rinaldo, A., 2007. Biologically-controlled multiple equilibria of tidal landforms and the fate of the Venice lagoon. Geophysical Research Letters 34, L11402.

Meehl, G.A., Washington, W.M., Collins, W.D., Arblaster, J.M., Hu, A.X., Buja, L.E., Strand, W.G., Teng, H.Y., 2005. How much more global warming and sea level rise? Science 307, 1769–1772.

Millennium Ecosystem Assessment, 2005. Ecosystems and human well-being: current state and trends. Island Press, Washington.

Morris, J.T., Sundareshwar, P.V., Nietch, C.T., Kjerfve, B., Cahoon, D.R., 2002. Responses of coastal wetlands to rising sea level. Ecology 83, 2869–2877.

Mudd, S.M., D'Alpaos, A., Morris, J.T., 2010. How does vegetation affect sedimentation on tidal marshes? Investigating particle capture and hydrodynamic controls on biologically mediated sedimentation. Journal of Geophysical Research 115, F03029.

Nicholls, R.J., 2004. Coastal flooding and wetland loss in the 21st century: changes under the SRES climate and socio-economic scenarios. Global Environmental Change 14, 69–86.

Nicholls, R.J., Cazenave, A., 2010. Sea-level rise and its impact on coastal zones. Science 328, 1517–1520.

Resio, D.T., Westerink, J.J., 2008. Modelling the physics of storm surges. Physics Today 61, 33–38.

Silliman, B.R., Van de Koppel, J., Bertness, M.D., Stanton, L.E., Mendelssohn, I.A., 2005. Drought, snails, and large-scale die-off of southern U.S. salt marshes. Science 310, 1803–1806.

Stokstad, E., 2005. After Katrina–Louisiana's wetlands struggle for survival. Science 310, 1264–1266.

Temmerman, S., Bouma, T.J., Govers, G., Wang, Z.B., De Vries, M.B., Herman, P.M.J., 2005. Impact of vegetation on flow routing and sedimentation patterns: three-dimensional modeling for a tidal marsh. Journal of Geophysical Research 110, F04019.

Temmerman, S., Bouma, T.J., Van de Koppel, J., Van der Wal, D., De Vries, M.B., Herman, P.M.J., 2007. Vegetation causes channel erosion in a tidal landscape. Geology 35, 631–634.

Wamsley, T.V., Cialone, M.A., Smith, J.M., Ebersole, B.A., Grzegorzewski, A.S., 2009. Influence of landscape restoration and degradation on storm surge and waves in southern Louisiana. Natural Hazards 51, 207–224.

Wamsley, T.V., Cialone, M.A., Smith, J.M., Atkinson, J.H., Rosati, J.D., 2010. The potential of wetlands in reducing storm surge. Ocean Engineering 37, 59–68.

Webster, P.J., Holland, G.J., Curry, J.A., Chang, H.R., 2005. Changes in tropical cyclone number, duration, and intensity in a warming environment. Science 309, 1844–1846.

Westerink, J.J., Luettich, R.A., Feyen, J.C., Atkinson, J.H., Dawson, C., Roberts, H.J., Powell, M.D., Dunion, J.P., Kubatko, E.J., Pourtaheri, H., 2008. A basin- to channel-scale unstructured grid hurricane storm surge model applied to southern Louisiana. Monthly Weather Review 136, 833–864.